ACS OMEGA

Open Access

http://pubs.acs.org/journal/acsodf

Article

Poloxamer 407 Combined with Polyvinylpyrrolidone To Prepare a High-Performance Poly(ether sulfone) Ultrafiltration Membrane

Zhijiang Sun,[§] Zehua Yin,*[,§] Mingyu Zhang, Dongli Guo, and Fen Ran*

Cite This: *ACS Omega* 2023, 8, 39783−39795

Read Online

ACCESS | Metrics & More | Article Recommendations | Supporting Information

ABSTRACT: At present, the design and fabrication of polymer membranes with high permeability and good retention ability are still huge challenges. In this study, the commercial Poloxamer 407 (Pluronic F127) is selected as a multifunctional additive, and polyvinylpyrrolidone is used as a pore-forming agent to modify the poly(ether sulfone) membrane by liquid−liquid phase conversion technology to prepare an ultrafiltration membrane with excellent performance. The hydrophobic poly(propylene oxide) segment in Poloxamer 407 guarantees that this copolymer can be firmly anchored to the poly(ether sulfone) matrix, and the hydrophilic poly(ethylene oxide) segments in Poloxamer 407 impart a stronger hydrophilic nature to the modified membrane surface. Therefore, the permeability and hydrophilicity of the modified membrane are significantly improved and the modified membrane also has good stability. When the amount of Poloxamer 407 added to the casting solution reached 0.6 g, the water flux of the modified membrane was as high as 368 L m^{-2} h^{-1}, and the rejection rate of bovine serum albumin was close to 98%. In the test to isolate organic small molecule dyes, the retention rate of the modified membrane to Congo red is 94.27%. In addition, the modified membrane shows an excellent water flux recovery rate and antifouling ability. It performs well in subsequent cycle tests and long-term membrane life tests and can be used repeatedly. Our work has resulted in poly(ether sulfone) membranes with good performance, which show great potential in the treatment of biomedical wastewater and the removal of industrial organic dye wastewater, it provides ideas for the development and application of amphiphilic polymer materials.

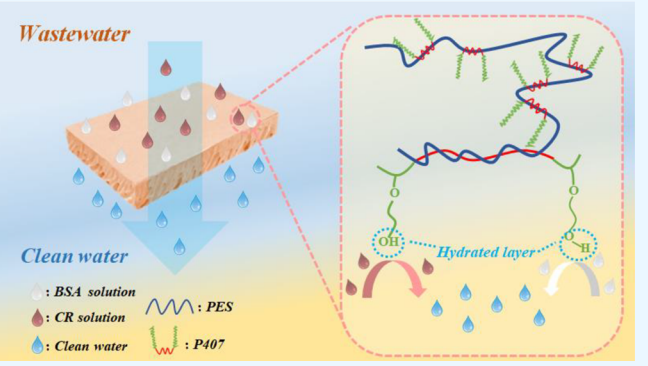

INTRODUCTION

Since the beginning of the 21st century, with the rapid development of the economy and the rapid increase in the number of human beings, problems such as a sharp decline in resources, energy shortages, and environmental pollution have become increasingly prominent.[1] Membrane separation technology with its unique technical characteristics and high efficiency and economic advantages has gradually become the key to solving the above problems.[2,3] At present, membrane separation technology has made significant progress in both research and industrial production;[4] it has been widely used in industrial wastewater treatment, biomedicine, seawater desalination, food processing, drug purification, and other fields.[5−7] Commonly used membrane materials are mainly divided into organic and inorganic membranes. Among them, organic polymers have been widely used in the separation of membrane materials because of their simple preparation process, low cost, and rich variety.[8] Commonly used polymer membrane materials are polyacrylonitrile, polyimide, cellulose, poly(ether sulfone), poly(vinylidene fluoride), polysulfone, etc. Among them, poly(ether sulfone) (PES) is a widely used polymer membrane material due to its good thermal, physical, chemical, and mechanical properties.[9−12]

However, the common problems and disadvantages of some polymer-based membrane materials are the same.[13] Due to its hydrophobicity, poly(ether sulfone) is easily contaminated by the nonspecific adhesion of proteins and other contaminant molecules. When used for wastewater purification, the adhesion of proteins or other contaminant molecules on the membrane surface and membrane pore surface can block the transport channels of the membrane, thereby reducing its permeation flux and stability during filtration.[14] In particular, for hemodialysis membranes, excessive protein adsorption and platelet adhesion will lead to the formation of blood clots, which in turn will adversely affect human health.[15−17] Moreover, the surface hydrophobicity of the membrane is not conducive to the penetration of water and the removal of

Received: August 8, 2023
Accepted: September 21, 2023
Published: October 11, 2023

the corresponding molecules, which will cause a low purification efficiency of the membrane.

To overcome the defects of the poly(ether sulfone) membrane material itself, many methods have been developed, which can be divided into internal modification and surface modification according to their different positions.[18] The internal modification methods mainly include blending modification, bulk modification, plasticizer extraction modification, etc.[19−21] The modification methods of the surface mainly include surface coating, surface grafting, plasma treatment, interface polymerization, etc.[22−24] However, most of these methods are not satisfactory for industrial-scale applications. The method is simple and low-cost and does not cause damage to the structure of the membrane itself, which is the most convenient and concise method.

Specific modifiers are added to membrane casting fluids, such as commonly used hydrophilic polymers, including polyethylene glycol (PEG), polyvinylpyrrolidone (PVP), and poly(vinyl alcohol) (PVA), inorganic nanoadditives such as nanotitanium dioxide, nanosilica, carbon nanotubes, and graphene nanomaterials.[25−30] Compared to the two, typical hydrophilic polymers, such as PVP and PEG are highly hydrophilic. In the NIPS process, pores are easy to extract from the solid membrane surface, and they are often used for hydrophobic membrane modification to significantly improve the wettability of the membrane surface. Due to its difficult-to-control branched structure, it is easy to come out of the membrane, and mixing with the membrane matrix will produce an uneven pore structure, thereby affecting the screening performance of the membrane.[31−34] However, the poor binding ability of inorganic nanomaterials to matrix materials will lead to unstable membrane modification.

Self-organizing blends containing hydrophilic and hydrophobic polymer segments are introduced,[35,36] such as amphiphilic block copolymers that rely on their properties to solve the shortcomings of the above-mentioned hydrophilic polymer additives and inorganic nanoadditives to modify poly(ether sulfone) membranes. The poly(ethylene oxide) (PEO-PPO-PEO) triblock copolymer is a typical amphiphilic block copolymer with hydrophobic PPO segments and hydrophilic PEO segments.[37] The poly(ether sulfone) (PES)/Pluronic F127 blend prepared by Jiang et al. showed satisfactory performance.[38] During the NIPS phase conversion process, Poloxamer 407 molecules are more likely to be enriched on the membrane surface due to their hydrophilic poly(ethylene oxide) (PEO) long chains, giving the membrane surface stronger wettability, and the strong interaction between the hydrophobic poly(propylene oxide) (PPO) segment and the hydrophobic matrix makes the copolymer firmly fixed on the PES matrix. Jiang et al. studied the effect of F-127 on the permeability of PES-modified ultrafiltration membranes and found that F-127 could be stably present in the blended membrane and that PES and F-127 showed partial miscibility by differential scanning calorimetry (DSC).[39] It is worth mentioning that the Flory−Huggins interaction parameter can be used to describe the compatibility between different polymers for the result of the hydrophobic PPO segment on F-127 being miscible with PES.[40] For two polymers that can be miscible, a sufficiently beneficial interaction polymer solution can form a mixing coil. In this case, it is possible to reduce the Gibbs energy of the system by combining one polymer coil and another polymer molecule into an isolated coil.[41] In previous studies, Pluronic F127's effects were only considered a surface modifier.[42] However, Jiang et al. later found that the addition of Pluronic F127 can also significantly increase the permeability of cellulose acetate ultrafiltration membranes, and the role of Pluronic F127 in this work is regarded as a pore-forming agent.[43] It is worth considering that adding Poloxamer 407 as an additive to the membrane matrix can significantly reduce protein adsorption or platelet adhesion on the surface of the blended membrane, the separation performance will hardly change, this also provides ideas for the efficient treatment of biomedical wastewater.[44−46] Although amphiphilic polymers can optimize the hydrophilic, antifouling, and biocompatible performance of ultrafiltration membranes at the laboratory level,[47] the development of amphiphilic polymer blended membrane materials is limited by the scarcity of raw materials, the difficulty of large-scale production, and the control of membrane-forming process, and it is difficult to achieve successful application in commercial factories.

In this study, we used PES as the polymer membrane matrix and PVP as the pore-forming agent and P407 as a multifunctional additive. By changing the polymer matrix and the amount of P407 added to the modified membrane, we prepared a series of M-PES/P407 ultrafiltration membranes with improved permeation flux and high antifouling performance. The permeation flux of the prepared modified membrane is controllable, which changes with the change of the content of each component in the casting solution, while the modified membrane maintains a high molecular retention rate, enhanced antipollution ability, and long cycle stability and has a long service life.

The comprehensive analysis of experimental results shows that compared with single-porous PVP, P407 has the role of multifunctional additive and performs well, which opens up ideas for the development of amphiphilic polymer materials in the future and their application in commercial factories. The M-PES/P407-0.6 ultrafiltration membrane prepared with P407 and PVP as additives shows the potential for effective treatment of biomedical wastewater and industrial wastewater, which is of great significance for the future development of water treatment and even hemodialysis technology.[48,49]

EXPERIMENTAL SECTION

Chemicals and Materials. Poly(ether sulfone) (PES, Ultrason E6020P, M_w = 58,000 Da) was purchased from BASF, Germany. Poloxamer 407(P407) was purchased from Jiangsu Care Medical Technology Co., Ltd. (Suzhou, China). Polyvinylpyrrolidone (PVP, M_w = 58,000 g/mol) was purchased from Shanghai Macklin Biotechnology Co., Ltd. (Shanghai, China). N, N-dimethylacetamide (DMAc; AR, purity 99.0%) was purchased from Sinopharm Chemical Reagent Co., Ltd. (Shanghai, China) and used as the solvent. Bovine serum albumin (BSA, M_w = 67 kDa) and congo red (CR, M_w = 696 Da) were purchased from Aladdin Reagent Co., Ltd. All other reagents (analytical grade) were obtained from Sinopharm Chemical Reagent Co., Ltd., China, and used without further purification. Ultrapure water was prepared in a laboratory.

Preparation of PES and M-PES/P407 Membrane. The P407-modified PES membrane was prepared as follows: A certain mass fraction of P407 was added into DMAc. After P407 was completely dispersed, a certain mass fraction of PES and 0.1 g of pvp were then added to the mixture, which was stirred at room temperature for 12 h to obtain a homogeneous

https://doi.org/10.1021/acsomega.3c05845
ACS Omega 2023, 8, 39783−39795

solution. After that, the uniform casting solution was degassed for 4 h and spread on a clean glass surface. The thickness of the membrane can be adjusted by scraping, and a certain amount of casting solution is evenly applied to the glass plate. The scraper thickness of the scraped blade is 150 μm, and the coating distance is 35 cm. The glass plate with the casting solution is then quickly placed in DI water; stable membranes were prepared by the method of nonsolvent-induced phase separation (NIPS). To completely remove the solvent DMAc, a stable membrane needs to be immersed in DI water for more than 48 h. Different membranes were prepared by changing the content ratios of PES, PVP, and P407. Specific ingredients can be found in Table 1.

Table 1. Casting Solution Composition for Different Membranes

samples	PES (g)	PVP (g)	DMAC (mL)	P407 (g)
PES	1.8	0	8.2	0
M-PES	1.7	0.1	8.2	0
M-PES/P407-0.2	1.5	0.1	8.2	0.2
M-PES/P407-0.4	1.3	0.1	8.2	0.4
M-PES/P407-0.6	1.1	0.1	8.2	0.6
M-PES/P407-0.8	0.9	0.1	8.2	0.8

Characterizations. The top surface and cross-sectional morphologies of the membrane were characterized by scanning electron microscopy (SEM, JSM-6700F JEOL, Japan), and the membranes were fractured in liquid nitrogen to obtain their cross-sectional structure. Fourier transform infrared (FTIR) spectra were tested in the 4000−650 cm^{-1} wavenumber region (Thermo Nicolet 6700, Thermo Fisher, USA). A thermogravimetric analysis (TGA, STA 6000, PerkinElmer, USA) was performed between 30 and 800 °C in air to assess the carbonaceous species weight percent. A SHIMADZU UV-3600 Plus UV spectrophotometer was used for measuring UV−vis absorption spectra. The hydrophilicity of the surface of the modified membrane was tested by the contact angle analyzer (WCA, PHS-3C, Precision Science Co., Shanghai, China). The porosity of the membrane was analyzed by an Electronic analytical balance (FA 2004).

Membrane porosity ε (%): ε (%) was the ratio of the total volume of pores to the total volume of the membrane.[50] In this article, it was determined by the dry-wet weight method. The membrane was cut into a size of 5 cm × 5 cm, dried at 60 °C, immersed in DI water at 25 °C for 48 h, dried, and, weighed. Porosity ε (%) was calculated by

$$\varepsilon = \frac{w_1 - w_2}{A \times l \times \rho_w} \tag{1}$$

where ε (%) was the porosity of the membrane, W_1 (g) was the wet membrane mass, W_2 (g) was the dry membrane mass, A (m^2) was the area of the membrane, l (m) was the thickness of the membrane, and ρ (0.987 g cm^{-3}) was the density of DI water at 25 °C. The average value is obtained by repeated three measurements.

Mean pore size test: The mean pore size (r_m) of the original membrane and the modified membrane was measured using the filtration velocimetry method in the literature and calculated using the Guerout-Elford-Ferry equation[51]:

$$r_m = \sqrt{\frac{(2.9 - 1.75\varepsilon) \times 8 \times \eta \times l \times Q}{\varepsilon \times A \times \Delta P}} \tag{2}$$

Among them, ε is the porosity of the membrane, η is the viscosity of water (8.9×10^{-4} Pa s), A is the membrane area (m^2), l is the thickness of the membrane (m), Q is the volume of permeation solution per unit time (m^3 s^{-1}), and ΔP is the membrane filtration pressure (0.1 MPa).

Membrane Performance Test. Flux refers to the volume of fluid passing through a membrane per unit of time and per unit area. The retention rate refers to the retention rate of the membrane to the solute as a percentage of the total solute, reflecting the selective separation of a substance by the test membrane.

Test of membrane flux, flux recovery ratio, and antifouling performance: First, a cross-flow filtration device with an effective area of 23.7 cm^2 was used to test the membrane performance at room temperature. Then, the membrane was prepressed at 0.2 MPa for 30 min and adjusted to 0.1 MPa for the pure water flux test. It was measured the permeate volume was every 10 min and repeated 6 times. Pure water flux (J_{W1}) was calculated by eq 3. After testing the pure water flux for 1 h, replace the pure water in the instrument with a BSA or CR solution (BSA solution is used to simulate biological wastewater, CR solution (0.2 g L^{-1}) was used to simulate organic dye CR wastewater). The specific test conditions and methods are the same as those of pure water tests. During the test, an appropriate amount of permeate is collected for ultraviolet−visible (UV−vis) spectroscopy. The BSA or CR flux (J_p) is calculated by eq 3. According to eqs 4−7, the flux recovery ratio (FRR), total fouling ratio (R_t), reversible fouling ratio (R_r), and irreversible fouling ratio (R_{ir}) were calculated, respectively.

$$J_W = \frac{V}{S \times t} \tag{3}$$

where V (L) is the volume of permeate; S (m^2) is the effective test area; and t (h) is the test time.

$$\mathrm{FRR} = \frac{J_{W2}}{J_{W1}} \times 100\% \tag{4}$$

$$R_t = \left(1 - \frac{J_p}{J_{W1}}\right) \times 100\% \tag{5}$$

$$R_r = \frac{J_{W2} - J_p}{J_{W1}} \times 100\% \tag{6}$$

$$R_{ir} = \left(1 - \frac{J_{W2}}{J_{W1}}\right) \times 100\% \tag{7}$$

Among them, J_{W1} (L m^{-2} h^{-1}) is the first pure water flux; J_{W2} (L m^{-2} h^{-1}) is the second recovery water flux; and J_P (L m^{-2} h^{-1}) is the flux of the BSA solution or CR solution.

Membrane retention tests were performed using BSA or CR solutions, the feed solution and permeate solution were measured by UV−vis, and the corresponding concentrations were calculated. The Retention rate (R) is calculated by eq 8.

$$R = \left(1 - \frac{C_p}{C_f}\right) \times 100\% \tag{8}$$

https://doi.org/10.1021/acsomega.3c05845
ACS Omega 2023, 8, 39783−39795

Scheme 1. Schematic Diagram of the Role of P407 and PVP in the Formation of Modified Membranes. (a) Three States of Pore-forming Agents PVP and P407 in a Uniform Casting Solution. (b) Formation of an Ordered Structure and Pores in the Modified Membrane by P407 and PVP

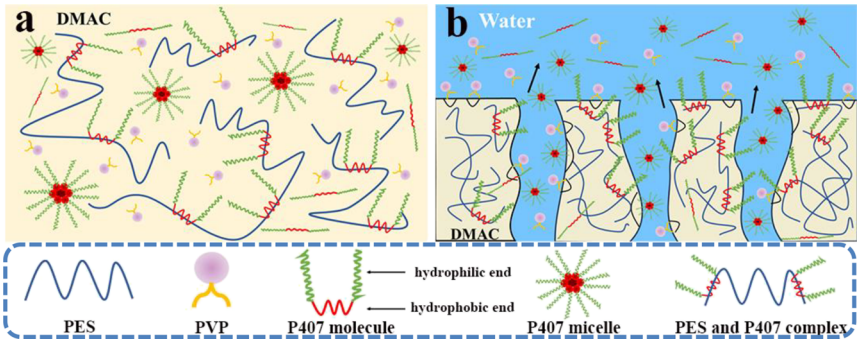

where C_p (g L^{-1}) was the concentration of the permeate solution, and C_f (g L^{-1}) was the concentration of the feed solution.

The long-term life test of the membrane is carried out every day, such as 2 h in pure water, test in BSA solution for 2 h, and finally, washing the membrane with DI water for 3 h. The daily pure water flow, BSA flow rate, and retention rate, respectively, are calculated; the duration of the test is 1 week. For the long-term life test of the membrane in CR solution, the process is the same as that described above.

RESULTS AND DISCUSSION

Poly(ether sulfone) (PES), polyvinylpyrrolidone (PVP), and poloxamer 407 (P407) are dissolved in *N, N*-dimethylacetamide (DMAC) according to different additions, and a series of modified membranes are prepared by liquid−liquid separation phase conversion. The preparation process of the modified membrane is shown in (Figure S1 in Supporting Information). Among them, PES is a polymer matrix material, PVP is a pore-forming agent, and P407 is a multifunctional modification additive. The use of P407 as a multifunctional additive for PES membrane modification improves the permeation flux and antifouling ability of the modified membrane and gives the modified membrane an improved water flux recovery rate, as well as maintaining a high retention rate for the permeation solution and the stability of the modified membrane.

During the phase conversion of NIPS, the strong interaction between the coagulation bath water and the hydrophilic poly(ethylene oxide) (PEO) segment rich in many hydroxyl groups on P407 leads to the tendency of P407 molecules to migrate outside the membrane and dissolve in the coagulation bath. At the same time, with the solidification of the liquid membrane in the coagulation bath, the migration resistance of P407 molecules increased rapidly, thereby inhibiting the migration and loss of the molecules. Such two interactions will cause more P407 to be fixed in the surface cortex of the membrane, and its hydrophobic poly(propylene oxide) (PPO) segment will strongly tend to be combined by hydrophobic PES cleavage so that its hydrophobic part is embedded in PES, which will give the membrane better overall stability.[52,53] The hydrophilic PEO segment on P407 extends to the outside of the membrane to form a catenary, which gives the modified membrane better wettability and antifouling ability.

The hydrophobic poly(ether sulfone) is modified by amphiphilic P407 and porous PVP. From an analytical point of view, the role of PVP on the modified PES membrane is relatively simple, mainly for the process of impregnating the sinking phase into a membrane to come out, plays the role of porogen, and its mechanism of action is similar to the third point of the influence of P407 on the membrane formation process described below. The addition of P407 to the casting solution may have a more complex effect on the membrane formation process, which can be roughly manifested in three ways, as shown in Scheme 1. First, there is the formation of PES/Pluronic aggregation. The hydrophobic PPO segments in P407 strongly tend to bind to PES cleavage, and this interaction results in P407 being wrapped around PES. Second, the effect of surface adsorption. P407 is amphiphilic, and DMAC (solvent) and water (nonsolvent) are hydrophilic; therefore, the formation of a P407 layer at the interface of the nonsolvent (water) and solvent (DMAC) phases will accelerate the diffusion rate of the nonsolvent phase. In the liquid−liquid separation phase conversion process, when the solvent in the casting solution first meets the nonsolvent in the solidification bath, most nonsolvents will be rapidly desolubilized into the casting solution; this will result in the growth of more nuclei in the porous sublayer and the formation of a high concentration of polymers. Third, the micellization of the P407 copolymer itself. Hydrophilic PEO fragments are usually confined to the outer layer (corona), while hydrophobic PPO fragments are distributed closer to the micelles (core). The formation of P407 micelles enables the flexible adjustment of the pore size of the dense layer of the prepared membrane. Since the addition of nonsolvent results in a change in the composition of the casting solution, the membrane casting system will cross the bimodal boundary into the unstable zone and the first nucleus of the P407 micelle will grow and appear, thus creating pores in the membrane surface. P407 micelles are also trapped in the surface layer during membrane formation. The mutual repulsion between the PES and P407 micelles will also lead to the appearance of a loose membrane surface. When hydrophilic P407 micelles are removed from the membrane by a nonsolvent, the area left behind after their removal also determines the pore size of the membrane. Therefore, the size of the formed P407 micelles will affect the pore radius of the membrane epidermis layer, and the pore structure change can be indirectly judged. Relevant studies have shown that the increasing concentration of P407 copolymer in nonsolvent solutions will cause a decrease in the critical micelle concentration (CMC), resulting in a gradual increase in the aggregation of P407 micelles.[54,55] Therefore, we can determine that the number of P407 micelles and the pore size of the membrane surface increase during phase conversion as the

https://doi.org/10.1021/acsomega.3c05845
ACS Omega 2023, 8, 39783−39795

concentration of P407 in the casting solution increases. Subsequent protein rejection and small organic molecule dye separation experiments as well as the determination of membrane porosity and average pore size provided additional support.

Figure 1 shows the surface morphologies and structures of the original and modified membrane. As can be seen from

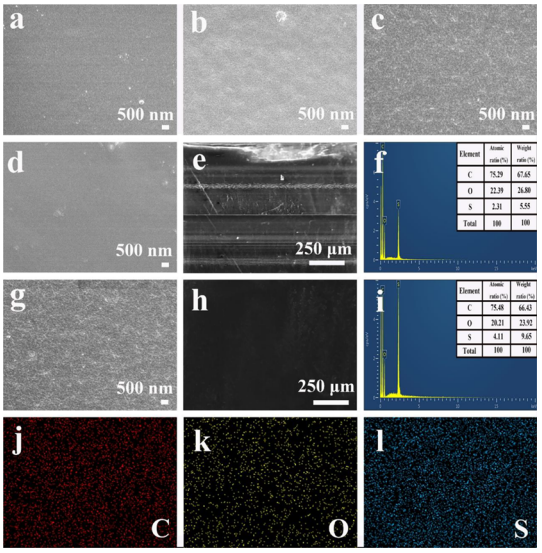

Figure 1. SEM images of (a) PES, (b) M-PES/P407-0.2, (c) M-PES/P407-0.4, (d) M-PES, and (g) M-PES/P407-0.6; (e, f) EDX spectrum of membranes of M-PES; (h, i) EDS mapping of membranes of M-PES/P407-0.6; and (j–l) three elements.

Figure 1, the surface of the original poly(ether sulfone) (PES) looks smooth, compact, flat, and free of folds (Figure 1 a). With the addition of 0.1 g of PVP, the surface of M-PES appears smoother and smoother (Figure 2d). In contrast, when changing the content of each component in the casting solution to prepare a series of M-PES/P407 membranes in different proportions, it can be observed that with the increase of P407, the surface of the membrane begins to fold, becoming less flat but still dense. The proportion of P407 in the casting solution increases, and the coarser the membrane surface becomes, with many small folds (Figure 1b,c,g). This phenomenon increases the effective area of the membrane and does not destroy the density of the membrane itself when the ratio of PES to P407 and PVP is maintained (Figure S2 in the Supporting Information). This surface morphology of the modified membrane not only increases the effective contact area with water and promotes the formation of the "hydrated layer" during the infiltration process but also changes the shape and morphology of the surface roughness of the membrane, and it is easier to intercept large-sized pollutant molecules. When the amount of P407 increases to 0.8 g, many holes in the hundreds of nanometers appear on the scanned electron microscopy images of M-PES/P407-0.8 (Figure S3 in the Supporting Information); the membrane is now at the microfiltration level. This shows that P407 has exceeded its maximum addition at this modified membrane ratio, and with the decrease of poly(ether sulfone) matrix addition, a larger proportion of P407 will form many micelles that will destroy the structure of the membrane itself. Comparing the energy dispersion spectra of M-PES and M-PES/P407-0.6, the results show that M-PES and M-PES/P407-0.6 are composed of three

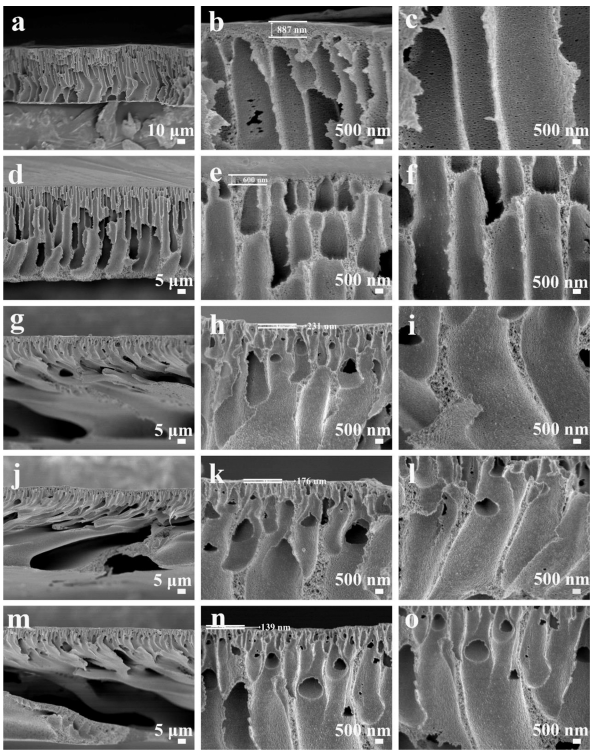

Figure 2. SEM images of cross-sectional views of (a–c) PES, (d–f) M-PES, (g–i) M-PES/P407-0.2, (j–l) M-PES/P407-0.4, and (m–o) M-PES/P407-0.6.

elements: C, O, and S (figures e,f and Figure h,i). Among them, the mass percentages of M-PES elements are 67.65, 26.8, and 5.55, while the mass percentages of M-PES/P407 elements are 66.43, 23.92, and 9.65, respectively. Comparing the two, it is found that no nitrogen is detected in the energy pigment spectra, and it also shows from the side that PVP completely plays the role of porosity and is completely removed in the liquid–liquid phase conversion process. The addition of poly(ether sulfone) to P407 is changed, resulting in a decrease in the proportion of O in M-PES/P407 compared with M-PES, which is also attributed to the large number of oxygen-containing functional groups in P407. With the change in the proportion of poly(ether sulfone) in the casting solution, the mass percentage of S in M-PES/P407-0.6 is also expected. The EDS mapping of the modified membrane M-PES/P407-0.6 is shown in (Figure 1 h,j–l). The results further show that the modified membrane contained C, S, and O elements on the surface and showed uniform distribution. These results show that P407 and PVP improve the effective contact area between the membrane surface and the permeate, and under the condition of a suitable ratio of casting solution, excellent compatibility with the membrane matrix is maintained.

Figure 2 shows the cross-sectional SEM micrographs of the pristine and modified PES membranes. It can be seen from the figure that the cross-section of the original membrane and the modified membrane present a typical finger-like pore asymmetric membrane structure. The top of the membrane cross-section is composed of a compact skin layer, the dense layer acts as a molecular sieve to play the role of a selective barrier, and the middle and lower parts are thick finger porelike structures, mainly providing mechanical support for the membrane. However, the thickness of the dense layer of the M-PES/P407 modified membrane changes with the change in

https://doi.org/10.1021/acsomega.3c05845
ACS Omega 2023, 8, 39783–39795

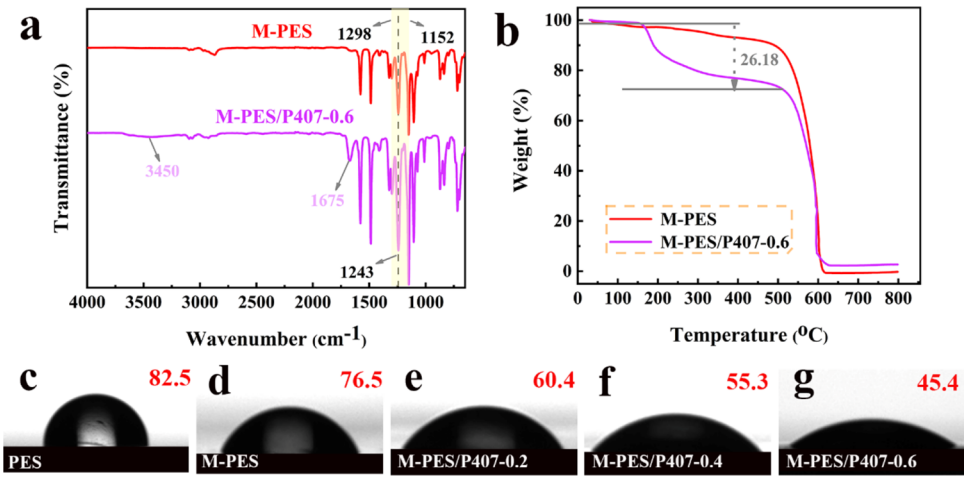

Figure 3. (a) FTIR spectra of M-PES and M-PES/P407-0.6. (b) TG curves of M-PES and M-PES/P407-0.6. (c−g) Average water contact angles on the top layer of membranes.

the content of each component in the casting solution. The thickness of PES is 887 nm, and after modification with the porous agent PVP, the thickness of M-PES is reduced to 600 nm. After adding P407 and changing the content of each component in the casting solution, the thickness of M-PES/P407 is reduced sequentially; among them, the thickness of M-PES/P407-0.6 is only 139 nm. The reduction of the thickness of the dense layer can reduce the transmission resistance of the permeate on the dense layer, thereby increasing the permeation flux of the membrane. In general, the flatter the dense layer of the membrane, the better the rejection performance. It can also be seen from the cross-sectional characterization that the dense layer of the modified membranes is flat and regular, so it has good retention performance.

At the same time, the finger hole of the modified membrane becomes larger, and the inner wall of the finger hole is more relaxed, with many spongy holes, larger holes at the several hundred nanometer levels begin to communicate on the inner wall of the finger hole, most prominently expressed by M-PES/P407-0.6. The size of the finger pore of the M-PES/P407 modified membrane increases with the increase of the mass fraction of P407, and the number and pore size of the large pores in the inner wall of the finger hole also increase. This phenomenon occurs because the PEO hydrophilic segments in P407 interact strongly with the deionized water in the solidification bath. This strong interaction will result in a strong exchange between the solvent and the nonsolvent in the solidification bath, increasing the phase separation rate and thus expanding the finger-like pore structure of the membrane. On the other hand, when the hydrophilic segment of the P407 migrates to the membrane surface, many spongy pores are formed on the inner wall of the membrane, and the hydrophobic chain segment is entangled with the molecular chain of PES to form a network structure, maintaining the integrity of the membrane structure. At the same time, as the concentration of P407 in the casting solution increases, the number of P407 micelles will increase and the formation of many hydrophilic micelles and their detachment from the membrane will result in the formation of large holes in the inner wall of the connecting finger hole. Therefore, the thinning of the dense layer of the modified membrane, the enlargement of the finger pores, and the emergence of more macropores connecting the inner wall of the finger pores are supported by the increase in the permeability of the modified membrane.

As shown in Figure 3, the functional groups on the membrane surfaces of M-PES and M-PES/P407-0.6 are confirmed by FTIR (Figure 3 a). The FTIR spectra of the test membrane show characteristic peaks at 1152 and 1298 cm^{-1}, which are attributed to the symmetrical and asymmetric O═S═O tensile vibrations of PES. The peak at 1243 cm^{-1} can be attributed to the asymmetric C−O−C tensile vibration of the PES substrate. When the infrared functional groups on the membrane surface were tested, the test membrane was dried at 60 °C to exclude the influence of the H_2O peak on the membrane surface. In the surface spectrum of the P407 modified membrane, the broad peak at 3450 cm^{-1} and the sharp characteristic peak at 1675 cm^{-1} indicated the O−H tensile vibration corresponding to P407. Analysis of infrared spectroscopy results showed that P407 had been successfully added to the modified membrane (Figure 3b). TG curves for M-PES and M-PES/P407. The TG curves are analyzed, and when the temperature rose to about 155 °C, P407 mixed in M-PES/P407-0.6 began to decompose by heat. In the temperature range of 155−510 °C, the weight of M-PES/P407-0.6 decreased by 26.18% relative to the initial moment. This result also confirms that a large amount of P407 in the M-PES/P407−0.6 membrane remains in the modified membrane after the NIPS process. Compared to M-PES, the addition of P407 will reduce the thermal stability of the poly(ether sulfone) matrix. At the same time, the TG curves are analyzed, and it is found that the amount of P407 lost by the modified membrane is less than the amount added to the corresponding casting solution. This result also validates our idea that part of P407 will be removed during the liquid−liquid phase separation to form a membrane, which plays the role of porosity. The value of the final sintered product of M-PES/P407-0.6 is 2.69%, while the value of the final product obtained by the TG curves of M-PES is negative, considering that the TG test is measured under air atmosphere conditions, and there are many influencing factors, but it is still in the normal error atmosphere. The wettability of the membrane surface is estimated by the water contact angle (WCA) as shown in (Figure 3c−g). In general, the wettability of the membrane surface is related to the hydrophilicity and porosity of the

https://doi.org/10.1021/acsomega.3c05845
ACS Omega 2023, 8, 39783−39795

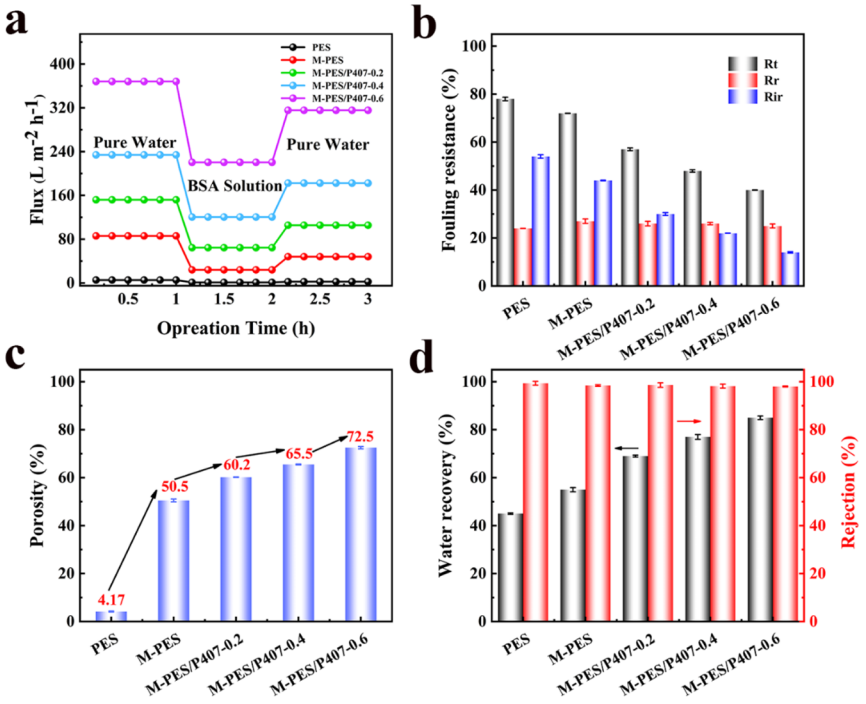

Figure 4. Performance of the modified membranes: (a) time-dependent flux, (b) fouling ratio, (c) overall porosity, (d) flux recovery ratios (FRR), and BSA rejection ratios.

membrane surface. The higher the hydrophilicity and porosity of the membrane surface, the smaller the water contact angle on the membrane surface. Due to the hydrophobicity of PES with a dense surface layer, the WCA of the original PES membrane is 82.5° (Figure 3C). The WCA of the modified membrane M-PES with 0.1 g of PVP is 76.5° (Figure 3d), indicating that the wettability of the membrane surface is enhanced. Compared with M-PES, the WCA of the P407 modified membrane changes with the increase of P407 content in the casting solution, and WCA gradually decreases. For M-PES/P407-0.6, the WCA on the membrane surface is reduced from 82.5° to 45.4° of the original PES membrane (Figure 3g); this indicates that the wettability of the modified membrane is enhanced. It can be noted that with the addition of P407 and PVP, the change of water contact angle on the membrane surface can effectively reduce the WCA and increase the wettability of the membrane. When the content of PVP in the casting solution is constant with the further improvement of the mass fraction of P407 in the modified membrane, the wettability of the membrane is further improved. This is mainly because P407 contains hydrophilic segments, which improve the interaction between water molecules and the membrane surface, and the pore-making role played by the additive P407 micellization, which increases the porosity of the membrane.

The ultrafiltration performance of the membrane can be observed, as shown in Figure 4. Figure 4a records the flux curve of pure water and BSA solution (simulated biomedical wastewater) over time after one cycle. It can be observed that with the addition of PVP and the increase of P407 content in the casting solution, the pure water flux of the modified membrane increases significantly. However, when the feed solution is replaced from pure water with the BSA solution, the permeation flux of the membrane decreases significantly. The main reason for this phenomenon is that when the feed solution is replaced with a BSA solution from pure water, a large number of BSA molecules will move to the membrane surface under pressure and BSA molecules with high molecular weight and large size are easy to adhere to the membrane surface, resulting in membrane pore blockage. After the membrane contaminated with the BSA solution is cleaned, the pure water flux test is performed again. Since the BSA molecular part adheres to the modified membrane and cannot be completely removed, the membrane pores are blocked, so the pure water flux of the membrane cannot be fully restored. The antifouling properties of the membrane are shown in (Figure 4b), and the total contamination rate (R_t) and irreversible contamination rate (R_{ir}) of the modified membrane decrease significantly as the proportion of P407 in the modified membrane increases. However, the reversible contamination rate (R_r) of the modified membrane increased with the increase of P407 content in the modified membrane mainly because the increase of hydrophilicity on the membrane surface would improve the fouling resistance of the membrane. The strong interaction between hydrophilic groups and water molecules on the modified membrane surface will promote the formation of a hydration layer on the membrane surface, thereby reducing the chance of BSA molecules being directly adsorbed on the membrane surface during the penetration test.

Therefore, the improvement of hydrophilicity on the membrane surface is conducive to improving the antifouling performance of the membrane and significantly prolonging the service life of the membrane. The effective porosity of the membrane has great influence on the permeability of the membrane. However, the porosity of the membrane can be achieved by changing the preparation conditions. (Figure 4c) shows the effect of P407 and PVP content on membrane porosity. The porosity of PES is only 4.17%, but with the addition of porous-forming agent PVP, the porosity of M-PES can reach 50.5%, and with the introduction of P407 as a multifunctional modifier, the porosity of M-PES/P407-0.6 is as

https://doi.org/10.1021/acsomega.3c05845
ACS Omega 2023, 8, 39783−39795

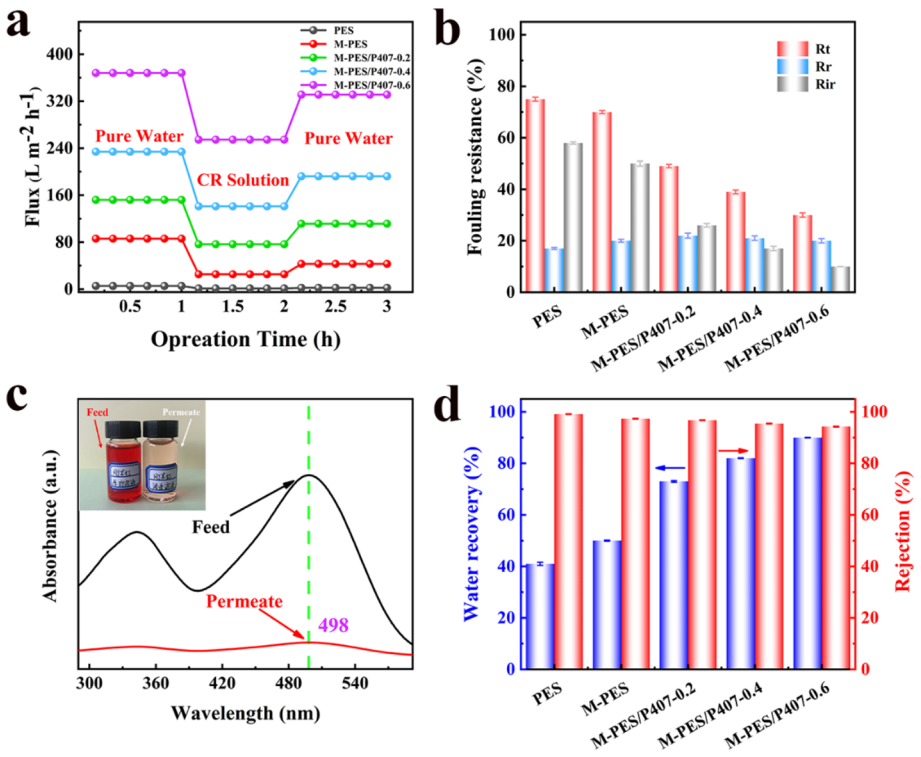

Figure 5. Performance of the modified membranes: (a) time-dependent flux, (b) fouling ratio, (c) UV absorption spectra of CR aqueous solution before and after filtration by M-PES/P407-0.6 (the illustration shows photos of stock solution (left) and permeate solution (right)), (d) FRR, and CR rejection ratios.

high as 72.5%. With the addition of PVP and P407, the mean pore size of M-PES increased to 11.23 nm compared with that of PES, the mean pore size of a series of modified membranes of M-PES/P407 also increased, and the mean pore size of M-PES/P407 reached 42.81 nm (Figure S4 in the Supporting Information). The increase in the average pore size of the modified membrane also explains the improvement in its permeability. Standard absorbance curve for BSA solution (Figure S5a in the Supporting Information). Taking the absorbance value as the ordinate and the BSA concentration (mg mL^{-1}) as the abscissa, the standard curve equation was fitted: $y = 0.5807x + 0.0093$, $R^2 = 0.998$. The concentration of the permeate is then calculated according to the absorbance standard curve of the BSA solution. Flux recovery (FRR) and BSA rejection are shown in Figure 4d. With the increase in P407 content in the M-PES/P407 membrane, the flux recovery rate of the modified membrane also increased significantly. In addition, the BSA retention rate of the modified membranes remained above 98%. From the above results, it can be observed that the modified membrane (M-PES/P407-0.6) can have greatly improved permeability and antifouling ability without sacrificing retention performance.

We use solute molecule CR of different sizes (simulated industrial dye wastewater) to continue to study the permeability and screening capacity of PES and the modified membranes, as shown in Figure 5. Figure 5a records the flux curve of pure water and the CR solution undergoing one cycle over time. It can be seen from the figure that the pure water flux of the modified membrane increases significantly with the increase of P407 content in M-PES/P407. The first water flux of PES is only 5.41 L m^{-2} h^{-1}, and the first water flux of M-PES prepared after PVP can reach 86 L m^{-2} h^{-1}, while the first water flux of M-PES/P407−0.6 reaches 368 L m^{-2} h^{-1}, and the first water flux of CR dye is 254.5L m^{-2} h^{-1}. After 2 h of membrane cleaning, the pure water flux returned to the first 331.2 L m^{-2} h^{-1}, indicating that the membrane had good water flux recovery. This is because the addition of P407 and PVP gives the modified membranes better hydrophilicity and higher porosity. The Modified membranes with stronger surface wettability and rich hydrophilic PEO segments will allow more water molecules to be "attracted" to the membrane surface, which can not only reduce the direct adsorption of CR molecules on the membrane surface but also increase the elution rate of contaminant molecules. The antifouling properties of the membrane are shown in (Figure 5b); and as the proportion of P407 in the casting solution increases, the total contamination rate (R_t) and irreversible contamination rate (R_{ir}) of the modified membrane continue to decrease, and the antifouling ability increases. As shown in Figure 5c, it is obvious that there is a very significant characteristic peak on the UV−vis spectral curve of the CR feed solution but almost no peak in the CR permeate solution. It can be seen from the color change of CR stock solution and permeate in physical photos that the content of CR molecules in permeate solution is greatly reduced. Similarly, the standard absorbance curve of the fitted CR solution is $y = 1.0318x + 0.01051$, $R^2 = 0.996$, and the CR concentration in the permeate is calculated according to the fitting curve (Figure S5b in the Supporting Information). Compared with the water flux test in the BSA solution shown in Figure 4, the modified membrane has a slightly higher antifouling ability for CR molecules than BSA molecules and M-PES/P407-0.6 maintains a water flux recovery rate of 90% and a high retention rate of 94.27% for CR molecules (Figure 5d). Figures 4 and 5 show that M-PES/P407-0.6 modified by P407 and PVP not only has good

https://doi.org/10.1021/acsomega.3c05845
ACS Omega 2023, 8, 39783−39795

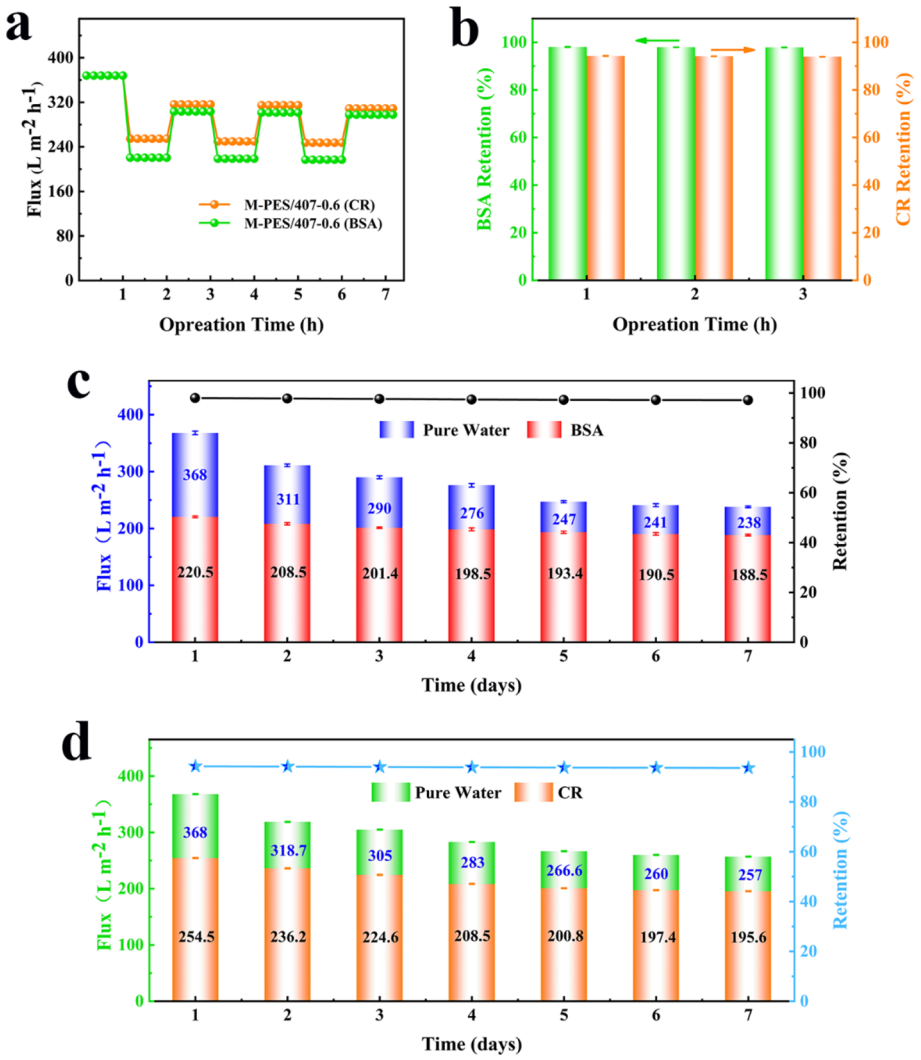

Figure 6. (a) Flux stability of M-PES/P407-0.6 during filtration of BSA and CR, (b) separation performance of M-PES/P407-0.6 on CR and BSA in aqueous solution, (c) long-term cycle stability performance of M-PES/P407-0.6 in BSA filtration, and (d) long-term cycle stability performance of M-PES/P407-0.6 in CR filtration.

application in biomedical wastewater but also has a high value for the treatment of traditional industrial dye wastewater.

As shown in Figure 6, as a qualified or even excellent ultrafiltration membrane, the cycle stability and long service life of the membrane are very important for practical applications. Figure 6a shows the flux stability test results for M-PES/P407-0.6, where CR and BSA are repeated at a pressure of 0.1 MPa. After the first flux test, the membrane reached a steady state without a change in water flux and recovery, indicating that the modified PES membrane had a good stability and recovery rate. In contrast, the water flux continues to decrease during flux stability testing of M-PES membranes (Figure S6 in the Supporting Information). This is mainly due to the strong adhesion of macromolecular solutes on the surface of the M-PES membrane, which is the result of the continuous accumulation of solute molecules during the test. In addition, the retention rate calculated by UV−vis detection of permeate is shown in the figure. In Figure 6b, the retention rate of the M-PES/P407-0.6 modified membrane remains unchanged, indicating that the membrane still had a good retention capacity under multiple cycles. As shown in Figure 6c, M-PES/P407-0.6 is subjected to long-term life testing in BSA. In the long-term life test, the initial pure water flux is 368 L m^{-2} h^{-1} and the BSA flux is 220.5 L m^{-2} h^{-1}. After several days of circulation, it was found that the BSA flux began to stabilize, the pure water flux reached a stable state, and the flux could remain at 238 L m^{-2} h^{-1}, without continuing to decline. This considers the excellent recovery properties of M-PES/P407-0.6. It should be noted that the decrease in pure water flux is mainly due to the membrane itself being contaminated with a small amount of BSA. In long-term life tests, the retention rate of BSA has been maintained above 97.2%. As shown in Figure 6d, M-PES/P407-0.6 is also tested for long life in CR solution, and the results are similar to those of the BSA solution. However, M-PES/P407-0.6 shows better resistance than BSA, with a CR flux of 254.5 L m^{-2} h^{-1}. Similarly, after a period of cycling, the CR flux gradually stabilized, the pure water flux gradually approached the limit value, and the flux remained at about 257 L m^{-2} h^{-1}. In long-term life testing, the retention rate of CR remains above 93.6%. Moreover, compared to the test in the process of filtering BSA, M-PES/P407 showed better results in the process of filtering CR. This is mainly due to the increase in membrane surface wettability and effective contact area, as well as the increase in the porosity and average

https://doi.org/10.1021/acsomega.3c05845
ACS Omega 2023, 8, 39783−39795

Table 2. Performance of Membranes with Different Additives in This Work and Literature

membrane	addictive	Water flux (L m^{-2} h^{-1})	rejection (%)	pressure (MPa)	ref
PES	DexPNI	118.5	BSA 97	0.1	10
PSF	PluronicF127	250	BSA 95	0.1	59
PES	Cu(tpa)@GO	140.0	CR 90	0.2	60
PES	PEI-TM-PES	72	BSA 91.4	0.1	61
PES	PVP/GO	28	BSA 90	0.4	62
PES	PES-*b*-PSBMA	115	BSA 80	0.1	63
PES	PES-*b*-PHEDMA	82	BSA 90	0.2	64
PES	TA-Ag	239.8	BSA 96.1	0.1	65
CA	MOF@GO	183	BSA 91.4	0.15	66
PSF	poly(AA-*co*-ACMO)	124.7	BSA 95	0.25	67
PES	Poloxamer 407/PVP	368	BSA 98CR 94.3	0.1	This work

pore size of the modified membrane, and the small size of organic dye molecules are easier to elute from the membrane than the test results in BSA solution. The above long cycle and stability tests show that P407 molecules have high stability in the modified membranes. This stability also derives mainly from the high migration resistance (kinetic factors) of the ternary block copolymer P407 molecule in solid systems and the strong interaction between its hydrophobic components and the hydrophobic matrix (thermodynamic factors).[56] Song et al. prepared a surface-functionalized polyethersulfone membrane by blending comb-like amphiphilic block copolymers and explained the stability enhancement of the modified membrane by using the principle that the hydrophobic segments of the amphiphilic block copolymer and the solubility parameters between the PES matrix were similar.[57] Surprisingly, in the subsequent study of poly(ether sulfone) in situ phase separation to prepare ultrathin hybrid membranes for highly flexible supercapacitors, Zhao et al. used the method of in situ preparation to make PES and AC generated by no new functional groups between each other. A homogeneous hybrid membrane was obtained by the strong combination of AC adsorption and PES, which maintained a good long-term cycle life and showed high stability.[58] In addition, we compare the performance of this work with membranes prepared with different kinds of additives[59−67] in other reports, as shown in Table 2. In general, the poly(ether sulfone) membrane modified by P407 and PVP showed good separation performance for CR and BSA and greatly increased the permeability and antifouling ability of the original membrane. The permeation flux increases while maintaining a high retention rate of the permeation solution as well as the long service life of M-PES/P407-0.6 and excellent cycling stability.

CONCLUSIONS

In summary, by simple blending, we add a certain amount of the pore-forming agent PVP to the casting solution and adjust the content of both the multifunctional additive P407 and the polymer matrix PES. A series of M-PES/P407 modified membranes are prepared by liquid−liquid-separated phase conversion. The experimental results confirm that amphiphilic P407 can be stably present in the blended membrane, and the surface wettability and effective contact area of the membrane are significantly improved. The prepared modified membrane (M-PES/P407-0.6) not only has high permeability (pure water flux of 368 L m^{-2} h^{-1}) and good separation capacity (BSA retention rate and CR retention rate of 98.02 and 94.27%, respectively), with high antifouling performance and long service life, which can be used in future separation processes involving environmental applications. It provides ideas for the development and application of amphiphilic polymer blended membrane materials in the future.

ASSOCIATED CONTENT

Supporting Information

The Supporting Information is available free of charge at https://pubs.acs.org/doi/10.1021/acsomega.3c05845.

Schematic diagram of the preparation process of P407 modified poly(ether sulfone) membrane; SEM images of membrane surface; SEM images of M-PES/P407-0.8 membrane surface; mean pore size (nm) of the modified membranes; (a) standard curves of bovine serum protein solution, and (b) standard curves of Congo red solution; (a) flux stability of the M-PES during filtration of BSA and CR, (b) separation performance of M-PES for CR and BSA in water solution (PDF)

AUTHOR INFORMATION

Corresponding Authors

Zehua Yin − *Jiangsu Solicitude Medical Technology co., Ltd., Suzhou 215100, PR China*; Email: yinzehua@smtworld.com

Fen Ran − *State Key Laboratory of Advanced Processing and Recycling of Non-ferrous Metals, School of Materials Science and Engineering, Lanzhou University of Technology, Lanzhou 730050, PR China*; orcid.org/0000-0002-7383-1265; Email: ranfen@lut.edu.cn

Authors

Zhijiang Sun − *State Key Laboratory of Advanced Processing and Recycling of Non-ferrous Metals, School of Materials Science and Engineering, Lanzhou University of Technology, Lanzhou 730050, PR China*

Mingyu Zhang − *State Key Laboratory of Advanced Processing and Recycling of Non-ferrous Metals, School of Materials Science and Engineering, Lanzhou University of Technology, Lanzhou 730050, PR China*

Dongli Guo − *State Key Laboratory of Advanced Processing and Recycling of Non-ferrous Metals, School of Materials Science and Engineering, Lanzhou University of Technology, Lanzhou 730050, PR China; Jiangsu Solicitude Medical Technology co., Ltd., Suzhou 215100, PR China*

Complete contact information is available at: https://pubs.acs.org/10.1021/acsomega.3c05845

https://doi.org/10.1021/acsomega.3c05845
ACS Omega 2023, 8, 39783−39795

Author Contributions

[§]Z.S. and Z.Y. contributed equally to this work.

Notes

The authors declare no competing financial interest.

■ ACKNOWLEDGMENTS

This work was partly supported by the National Natural Science Foundation of China (51763014 and 52073133), Key Talent Project Foundation of Gansu Province, Joint fund between Shenyang National Laboratory for Materials Science and State Key Laboratory of Advanced Processing and Recycling of Nonferrous Metals (18LHPY002), the Program for Hongliu Distinguished Young Scholars in Lanzhou University of Technology, and the Incubation Program of Excellent Doctoral Dissertation-Lanzhou University of Technology.

■ REFERENCES

(1) Ma, M.; Zhang, C.; Zhu, C.; Huang, S.; Yang, J.; Xu, Z. Nanocomposite membranes embedded with functionalized MoS_2 nanosheets for enhanced interfacial compatibility and nanofiltration performance. *J. Membr. Sci.* **2019**, *591*, No. 117316.

(2) Zhang, S.; Liu, Y.; Li, D.; Wang, Q.; Ran, F. Water-soluble MOF nanoparticles modified polyethersulfone membrane for improving flux and molecular retention. *Appl. Surf. Sci.* **2020**, *505*, No. 144553.

(3) Xu, Z.; Liao, J.; Tang, H.; Efome, J. E.; Li, N. Preparation and antifouling property improvement of Tröger's base polymer ultrafiltration membrane. *J. Membr. Sci.* **2018**, *561*, 59−68.

(4) Zhu, K.; Zhang, S.; Luan, J.; Mu, Y.; Du, Y.; Wang, G. Fabrication of ultrafiltration membranes with enhanced antifouling capability and stable mechanical properties via the strategies of blending and crosslinking. *J. Membr. Sci.* **2017**, *539*, 116−127.

(5) Zhu, J.; Zhang, Q.; Zheng, J.; Hou, S.; Mao, H.; Zhang, S. Green fabrication of a positively charged nanofiltration membrane by grafting poly(ethylene imine) onto a poly (arylene ether sulfone) membrane containing tertiary amine groups. *J. Membr. Sci.* **2016**, *517*, 39−46.

(6) Li, D.; Wu, J.; Yang, S.; Zhang, W.; Niu, X.; Chen, Y.; Ran, F. Hydrophilicity and anti-fouling performance of polyethersulfone membrane modified by grafting block glycosyl copolymers via surface initiated electrochemically mediated atom transfer radical polymerization. *New J. Chem.* **2018**, *42* (4), 2692−2701.

(7) Galanakis, C.; Fountoulis, G.; Gekas, V. Nanofiltration of brackish groundwater by using a polypiperazine membrane. *Desalination* **2012**, *286*, 277−284.

(8) Khan, A.; Sherazi, T. A.; Khan, Y.; Li, S.; Naqvi, S. A. R.; Cui, Z. Fabrication and characterization of polysulfone/modified nanocarbon black composite antifouling ultrafiltration membranes. *J. Membr. Sci.* **2018**, *554*, 71−82.

(9) Wei, R.; Guo, J.; Jin, L.; He, C.; Xie, Y.; Zhang, X.; Zhao, W.; Zhao, C. Vapor induced phase separation towards anion-/near-infrared-responsive pore channels for switchable anti-fouling membranes. *J. Mater. Chem. A* **2020**, *8* (18), 8934−8948.

(10) Li, D.; Niu, X.; Yang, S.; Chen, Y.; Ran, F. Thermo-responsive polysulfone membranes with good anti-fouling property modified by grafting random copolymers via surface-initiated eATRP. *Sep. Purif. Technol.* **2018**, *206*, 166−176.

(11) Liu, Y.; Tu, W.; Chen, M.; Ma, L.; Yang, B.; Liang, Q.; Chen, Y. A mussel-induced method to fabricate reduced graphene oxide/halloysite nanotubes membranes for multifunctional applications in water purification and oil/water separation. *Chem. Eng. J.* **2018**, *336*, 263−277.

(12) Du, X.; Wang, Z.; Liu, W.; Xu, J.; Chen, Z.; Wang, C. Imidazolium-functionalized poly (arylene ether ketone) cross-linked anion exchange membranes. *J. Membr. Sci.* **2018**, *566*, 205−212.

(13) Banerjee, I.; Pangule, R.; Kane, R. S. Antifouling coatings: recent developments in the design of surfaces that prevent fouling by proteins, bacteria, and marine organisms. *Adv. Mater.* **2011**, *23* (6), 690−718.

(14) Nie, C.; Yang, Y.; Peng, Z.; Cheng, C.; Ma, L.; Zhao, C. Aramid nanofiber as an emerging nanofibrous modifier to enhance ultrafiltration and biological performances of polymeric membranes. *J. Membr. Sci.* **2017**, *528*, 251−263.

(15) Zhang, Z.; Zhang, M.; Chen, S.; Horbett, T. A.; Ratner, B. D.; Jiang, S. Blood compatibility of surfaces with superlow protein adsorption. *Biomaterials* **2008**, *29* (32), 4285−4291.

(16) Andrade, J. D.; Hlady, V. Protein adsorption, and materials biocompatibility: A tutorial review and suggested hypotheses. *Adv. Polym. Sci.* **1986**, *79*, 1−63.

(17) Sun, S.; Yue, Y.; Huang, X.; Meng, D. Protein adsorption on blood-contact membranes. *J. Membr. Sci.* **2003**, *222* (1−2), 3−18.

(18) Ran, F.; Wu, J.; Niu, X.; Li, D.; Nie, C.; Wang, R.; Zhao, W.; Zhang, W.; Chen, Y.; Zhao, C. A new approach for membrane modification based on electrochemically mediated living polymerization and self-assembly of N-tert-butyl amide- and beta-cyclodextrin-involved macromolecules for blood purification. *Mater. Sci. Eng., C* **2019**, *95*, 122−133.

(19) Ran, F.; Nie, S.; Zhao, W.; Li, J.; Su, B.; Sun, S.; Zhao, C. Biocompatibility of modified polyethersulfone membranes by blending an amphiphilic triblock co-polymer of poly(vinyl pyrrolidone)-b-poly(methyl methacrylate)-b-poly(vinyl pyrrolidone). *Acta Biomater.* **2011**, *7* (9), 3370−3381.

(20) Yang, Q.; Chung, T.; Weber, M. Microscopic behavior of polyvinylpyrrolidone hydrophilizing agents on phase inversion polyethersulfone hollow fiber membranes for hemofiltration. *J. Membr. Sci.* **2009**, *326* (2), 322−331.

(21) Hallab, N. J.; Bundy, K. J.; O'Connor, K.; Clark, R.; Moses, R. L. Cell adhesion to biomaterials: correlations between surface charge, surface roughness, adsorbed protein, and cell morphology. *J. Long-Term Eff. Med. Implants* **1995**, *5* (3), 209−231.

(22) Esfahani, M. R.; Aktij, S. A.; Dabaghian, Z.; Firouzjaei, M. D.; Rahimpour, A.; Eke, J.; Escobar, I. C.; Abolhassani, M.; Greenlee, L. F.; Esfahani, A. R.; Sadmani, A.; Koutahzadeh, N. Nanocomposite membranes for water separation and purification: Fabrication, modification, and applications. *Sep. Purif. Technol.* **2019**, *213*, 465−499.

(23) Lin, Y.; Loh, C. H.; Shi, L.; Fan, Y. Q.; Wang, R. Preparation of high-performance Al_2O_3/PES composite hollow fiber UF membranes via facile in-situ vapor induced hydrolyzation. *J. Membr. Sci.* **2017**, *539*, 65−75.

(24) Xu, C.; Liu, X. J.; Xie, B. B.; Yao, C.; Hu, W. H.; Li, Y.; Li, X. S. Preparation of PES ultrafiltration membranes with natural amino acids based zwitterionic antifouling surfaces. *Appl. Surf. Sci.* **2016**, *385*, 130−138.

(25) Huang, J. X.; Yang, H. J.; Chen, M.; Ji, T.; Hou, Z. C.; Wu, M. H. An infrared spectroscopy study of PES PVP blend and PES-g-PVP copolymer. *Polym. Test.* **2017**, *59*, 212−219.

(26) Ran, F.; Song, H.; Wu, J. Y.; Ma, L.; Niu, X. Q.; Fan, H. L.; Kang, L.; Zhao, C. S. Bionic design for anticoagulant surface via synthesized biological macromolecules with heparin-like chains. *RSC Adv.* **2015**, *5* (71), 58032−58040.

(27) Xiang, T.; Wang, L. R.; Ma, L.; Han, Z. Y.; Wang, R.; Cheng, C.; Xia, Y.; Qin, H.; Zhao, C. S. From Commodity Polymers to Functional Polymers. *Sci. Rep.* **2014**, *4*, 4604.

(28) Chen, C.; Wang, J. M.; Liu, D.; Yang, C.; Liu, Y. C.; Ruoff, R. S.; Lei, W. W. Functionalized boron nitride membranes with ultrafast solvent transport performance for molecular separation. *Nat. Commun.* **2018**, *9*, 1920.

(29) Song, Z. N.; Fathizadeh, M.; Huang, Y.; Chu, K. H.; Yoon, Y.; Wang, L.; Xu, W.; Yu, M. TiO_2 nanofiltration membranes prepared by molecular layer deposition for water purification. *J. Membr. Sci.* **2016**, *510*, 72−78.

(30) Mavukkandy, M. O.; Zaib, Q.; Arafat, H. A. CNT/PVP blend PVDF membranes for the removal of organic pollutants from simulated treated wastewater effluent. *J. Environ. Chem. Eng.* **2018**, *6* (5), 6733−6740.

https://doi.org/10.1021/acsomega.3c05845
ACS Omega 2023, 8, 39783−39795

(31) Hassen, M. A.; Hamdy, G.; Sabry, R. M.; Ali, S. S.; Taher, F. A. Synthesis and characterization of PES/PSF/PEG by immersion precipitation for Mediterranean seawater desalination by FO membrane. *Polym. Eng. Sci.* **2023**, *63* (2), 509−520.
(32) Kourde-Hanafi, Y.; Loulergue, P.; Szymczyk, A.; Vander Bruggen, B.; Nachtnebel, M.; Rabiller-Baudry, M.; Audic, J.; Pölt, P.; Baddari, K. Influence of PVP content on degradation of PES/PVP membranes: Insights from characterization of membranes with controlled composition. *J. Membr. Sci.* **2017**, *533*, 261−269.
(33) Li, J.; Xu, Z.; Yang, H.; Feng, C.; Shi, J. Hydrophilic microporous PES membranes prepared by PES/PEG/DMAc casting solutions. *J. Appl. Polym. Sci.* **2008**, *107* (6), 4100−4108.
(34) Marbelia, L.; Bilad, M. R.; Vankelecom, I. F. J. Gradual PVP leaching from PVDF/PVP blend membranes and its effects on membrane fouling in membrane bioreactors. *Sep. Purif. Technol.* **2019**, *213*, 276−282.
(35) Hester, J. F.; Mayes, A. M. Design and performance of foul-resistant poly(vinylidene fluoride) membranes prepared in a single-step by surface segregation. *J. Membr. Sci.* **2002**, *202* (1), 119−135.
(36) Hester, J. F.; Banerjee, P.; Mayes, A. M. Preparation of Protein-Resistant Surfaces on Poly(vinylidene fluoride) Membranes via Surface Segregation. *Macromolecules* **1999**, *32* (5), 1643−1650.
(37) Zhao, W.; Su, Y. L.; Li, C.; Shi, Q.; Ning, X.; Jiang, Z. Y. Fabrication of antifouling polyethersulfone ultrafiltration membranes using Pluronic F127 as both surface modifier and pore-forming agent. *J. Membr. Sci.* **2008**, *318* (1−2), 405−412.
(38) Wang, Y. Q.; Wang, T.; Su, Y. L.; Peng, F. B.; Wu, H.; Jiang, Z. Y. Protein-adsorption-resistance and permeation property of polyethersulfone and soybean phosphatidylcholine blend ultrafiltration membranes. *J. Membr. Sci.* **2006**, *270* (1−2), 108−114.
(39) Wang, Y. Q.; Su, Y. L.; Sun, Q.; Ma, X.; Ma, X.; Jiang, Z. Y. Improved permeation performance of Pluronic F127−polyethersulfone blend ultrafiltration membranes. *J. Membr. Sci.* **2006**, *282* (1−2), 44−51.
(40) Van Leuken, S. H. M.; van Benthem, R. A. T. M.; Tuinier, R.; Vis, M. Predicting Multi-Component Phase Equilibria of Polymers using Approximations to Flory−Huggins Theory. *Macromol. Theory Simul.* **2023**, *32* (4), No. 2300001.
(41) Wolf, B. A. Intrinsic Viscosities of Polymer Blends and Polymer Compatibility: Self-Organization and Flory-Huggins Interaction Parameters. *Macromol. Chem. Phys.* **2018**, *219* (18), No. 1800249.
(42) Wang, Y. Q.; Wang, T.; Su, Y. L.; Peng, F. B.; Wu, H.; Jiang, Z. Y. Remarkable reduction of irreversible fouling and improvement of the permeation properties of poly(ether sulfone) ultrafiltration membranes by blending with pluronic F127. *Langmuir* **2005**, *21* (25), 11856−11862.
(43) Lv, C.; Su, Y.; Wang, Y.; Ma, X.; Sun, Q.; Jiang, Z. Enhanced permeation performance of cellulose acetate ultrafiltration membrane by incorporation of Pluronic F127. *J. Membr. Sci.* **2007**, *294* (1−2), 68−74.
(44) Kim, Y. W.; Shick Ahn, W.; Kim, J. J.; Ha Kim, Y. In situ fabrication of self-transformable and hydrophilic poly(ethylene glycol) derivative-modified polysulfone membranes. *Biomaterials* **2005**, *26* (16), 2867−2875.
(45) Park, J. Y.; Acar, M. H.; Akthakul, A.; Kuhlman, W.; Mayes, A. M. Polysulfone-graft-poly(ethylene glycol) graft copolymers for surface modification of polysulfone membranes. *Biomaterials* **2006**, *27* (6), 856−865.
(46) Hancock, L. F.; Fagan, S. M.; Ziolo, M. Hydrophilic, semipermeable membranes fabricated with poly(ethylene oxide)-polysulfone block copolymer. *Biomaterials* **2000**, *21* (7), 725−733.
(47) Liu, H.; Liu, Y.; Qin, Y.; Huang, Y.; Chen, K.; Xiao, C. Amphiphilic surface construction and properties of PVC-g-PPEGMA/PTFEMA graft copolymer membrane. *Appl. Surf. Sci.* **2021**, *545*, No. 148985.
(48) Saranya, R.; Arthanareeswaran, G.; Dionysiou, D. D. Treatment of paper mill effluent using Polyethersulfone/functionalized multi-walled carbon nanotubes based nanocomposite membranes. *Chem. Eng. J.* **2014**, *236*, 369−377.
(49) Nie, C. X.; Ma, L.; Xia, Y.; He, C.; Deng, J.; Wang, L. R.; Cheng, C.; Sun, S. D.; Zhao, C. S. Novel heparin-mimicking polymer brush grafted carbon nanotube/PES composite membranes for safe and efficient blood purification. *J. Membr. Sci.* **2015**, *475*, 455−468.
(50) Xu, M. H.; Xie, R.; Ju, X. J.; Wang, W.; Liu, Z.; Chu, L. Y. Antifouling membranes with bi-continuous porous structures and high fluxes prepared by vapor-induced phase separation. *J. Membr. Sci.* **2020**, *611*, No. 118256.
(51) Feng, C.; Shi, B. L.; Li, G. M.; Wu, Y. L. Preparation and properties of microporous membrane from poly(vinylidene fluoride-co-tetrafluoroethylene) (F2.4) for membrane distillation. *J. Membr. Sci.* **2004**, *237* (1−2), 15−24.
(52) Reining, Birte; Keul, Helmut; Höcker, Hartwig Amphiphilic block copolymers comprising poly(ethylene oxide) and poly(styrene) blocks: synthesis and surface morphology. *Polymer* **2002**, *43* (25), 7145−7154.
(53) Qin, J.; Wong, F.; Li, Y.; Liu, Y. A high flux ultrafiltration membrane spun from PSU/PVP (K90)/DMF/1,2-propanediol. *J. Membr. Sci.* **2003**, *211* (1), 139−147.
(54) Kozlov, M. Y.; Melik-Nubarov, N. S.; Batrakova, E. V.; Kabanov, A. Relationship between Pluronic Block Copolymer Structure, Critical Micellization Concentration and Partitioning Coefficients of Low Molecular Mass Solutes. *Macromolecules* **2000**, *33* (9), 3305−3313.
(55) Alexandridis, P.; Holzwarth, J. F.; Hatton, T. A. Micellization of Poly(ethylene oxide)-Poly(propylene oxide)-Poly(ethylene oxide) Triblock Copolymers in Aqueous Solutions: Thermodynamics of Copolymer Association. *Macromolecules* **1994**, *27* (9), 2414−2425.
(56) Zhao, J.; Zhang, P.; Cao, L.; Huo, H.; Lin, H.; Wang, Q.; Vogel, F.; Li, W.; Lin, Z. Amphiphilic Grafted Polymers Based on Citric Acid and Aniline Used to Enhance the Antifouling and Permeability Properties of PES Membranes. *Molecules* **2023**, *28* (4), 1936.
(57) Song, H.; Ran, F.; Fan, H.; Niu, X.; Kang, L.; Zhao, C. Hemocompatibility and ultrafiltration performance of surface-functionalized polyethersulfone membrane by blending comb-like amphiphilic block copolymer. *J. Membr. Sci.* **2014**, *471*, 319−327.
(58) Zhao, X.; Ran, F.; Shen, K.; Yang, Y.; Wu, J.; Niu, X.; Kong, L.; Kang, L.; Chen, S. Facile fabrication of ultrathin hybrid membrane for highly flexible supercapacitors via in-situ phase separation of polyethersulfone. *J. Power Sources* **2016**, *329*, 104−114.
(59) Plisko, T. V.; Penkova, A. V.; Burts, K. S.; Bildyukevich, A. V.; Dmitrenko, M. E.; Melnikova, G. B.; Atta, R. R.; Mazur, A. S.; Zolotarev, A. A.; Missyul, A. B. Effect of Pluronic F127 on porous and dense membrane structure formation via non-solvent induced and evaporation induced phase separation. *J. Membr. Sci.* **2019**, *580*, 336−349.
(60) Makhetha, T. A.; Moutloali, R. M. Antifouling properties of Cu(tpa)@GO/PES composite membranes and selective dye rejection. *J. Membr. Sci.* **2018**, *554*, 195−210.
(61) Lin, Z.; Hu, C.; Wu, X.; Zhong, W.; Chen, M.; Zhang, Q.; Zhu, A.; Liu, Q. Towards improved antifouling ability and separation performance of polyethersulfone ultrafiltration membranes through poly(ethylenimine) grafting. *J. Membr. Sci.* **2018**, *554*, 125−133.
(62) Zinadini, S.; Zinatizadeh, A. A.; Rahimi, M.; Vatanpour, V.; Zangeneh, H. Preparation of a novel antifouling mixed matrix PES membrane by embedding graphene oxide nanoplates. *J. Membr. Sci.* **2014**, *453*, 292−301.
(63) Zhao, Y.; Zhang, P.; Sun, J.; Liu, C.; Zhu, L.; Xu, Y. Electrolyte-responsive polyethersulfone membranes with zwitterionic polyethersulfone-based copolymers as additive. *J. Membr. Sci.* **2016**, *510*, 306−313.
(64) Zhao, Y.; Zhu, L.; Yi, Z.; Zhu, B.; Xu, Y. Zwitterionic hydrogel thin films as antifouling surface layers of polyethersulfone ultrafiltration membranes anchored via reactive copolymer additive. *J. Membr. Sci.* **2014**, *470*, 148−158.
(65) Fang, X.; Li, J.; Ren, B.; Huang, Y.; Wang, D.; Liao, Z.; Li, Q.; Wang, L.; Dionysiou, D. Polymeric ultrafiltration membrane with in situ formed nano-silver within the inner pores for simultaneous separation and catalysis. *J. Membr. Sci.* **2019**, *579*, 190−198.

https://doi.org/10.1021/acsomega.3c05845
ACS Omega 2023, 8, 39783−39795

(66) Yang, S.; Zou, Q.; Wang, T.; Zhang, L. Effects of GO and MOF@GO on the permeation and antifouling properties of cellulose acetate ultrafiltration membrane. *J. Membr. Sci.* **2019**, *569*, 48−59.
(67) Saini, B.; Khuntia, S.; Sinha, M. K. Incorporation of cross-linked poly(AA-co-ACMO) copolymer with pH responsive and hydrophilic properties to polysulfone ultrafiltration membrane for the mitigation of fouling behavior. *J. Membr. Sci.* **2019**, *572*, 184−197.

https://doi.org/10.1021/acsomega.3c05845
ACS Omega 2023, 8, 39783−39795